

B1 - Stress, strain and texture**B1 - O1****APPLICATIONS OF RESIDUAL STRESS DETERMINATION BY THE SPHERICAL HARMONICS MODEL****D. Balzar^{1,2} and N. C. Popa^{3,4}**¹*Department of Physics and Astronomy, University of Denver, Denver, CO 80208, USA*²*National Institute of Standards and Technology, Boulder, CO 80305, USA*³*Frank Laboratory of Neutron Physics, Joint Institute for Nuclear Research, 141980 Dubna, Moscow Region, Russia*⁴*National Institute for Materials Physics, P.O. Box MG-7, Bucharest, Romania*

The determination of residual strain/stress and texture through the spherical harmonics approach is becoming a route of choice for many researchers. The method can yield the full texture-weighted strain orientation distribution function for arbitrary crystal and sample symmetries. However, this approach requires the measurements of interplanar spacing of the several Bragg reflections at multiple sample orientations. Thus, energy-dispersive measurements and multiple detectors are very useful. We give an example of the neutron TOF measurements carried out at the LANSCE SMARTS station on the deformed uranium samples. We report the average macroscopic strain

and stress tensors, as applied to the orthorhombic crystal symmetry and general triclinic sample symmetry of the sample. The strain tensor was determined by the least-squares refinement of interplanar spacings for 19 Bragg reflections, as determined from the neutron TOF. An annealed uranium plate was used as a reference sample, thus providing reference interplanar spacings for all 19 reflections. The resulting strain and stress tensors show strong shear components that could not be detected through the measurements customary carried out along a few principal directions in the sample.

B1 - O2**NONUNIFORM SUBSTRUCTURE OF TEXTURED METAL MATERIALS: EXPERIMENTAL STUDY AND NEW-DISCOVERED REGULARITIES****Yuriy Perlovich, Margarita Isaenkova and Vladimir Fesenko***Moscow Engineering Physics Institute, Kashirskoe shosse 31, Moscow 115409, Russia*

Most data on the structure of metal materials, accessible by use of the standard X-ray methods, relate only to grains of some orientations, being in the reflecting position by X-ray measurements. Meantime, almost all technological treatments of metal materials lead to formation of specific crystallographic textures, so that metal becomes similar to a composite, whose components consist of grains with different orientations. Prehistories of these grains differ in plastic deformation mechanisms, trajectories of reorientation, strain hardening and, as a result, the substructure of textured material proves to be sharply inhomogeneous. In order to describe real metal materials from such point of view, a new efficient X-ray method of Generalized Pole Figures (GPF) was developed [1]. The method allows to obtain information about grains of all possible orientations and consists in diffractometric registration of the X-ray line profile by each successive position of the sample in the course of texture measurement, so that for planes $\{hkl\}$ of all orientations diffraction or substructure parameters are measured.

Obtained results are presented as GPF, that is distributions of measured and calculated X-ray diffraction or substructure parameters in the stereographic projection of the

sample depending on the orientation of reflecting crystallographic planes $\{hkl\}$. Among main diffraction parameters there are integral intensity I of the registered X-ray line (hkl), its angular position 2θ and the physical half-width β , fraction of the Gauss function in the approximated line profile; among substructure parameters, which can be calculated by X-ray data, – size of coherent domains D , interplanar spacing d_{hkl} , lattice distortion ϵ , dislocation density ρ and some others. The normalized GPF I_{hkl} is the usual texture pole figure $\{hkl\}$. The distribution of peak position GPF $2\theta_{hkl}$ can be recalculated into the distribution of lattice elastic deformation GPF d/d_{av} along crystallographic axes $\langle hkl \rangle$, where d_{av} - average weighted interplanar spacing and $d = d_{av} \pm \epsilon d_{av}$ with signs “+” or “-“ for cases of local elastic extension or contraction, respectively.

Since the physical half-width β_{hkl} depends on fragmentation of grains / distortion of their crystalline lattice and the peak position is determined by interplanar spacing along the normal to reflecting planes, GPF I_{hkl} and GPF $2\theta_{hkl}$ give the fullest accessible description of substructure, formed in textured metal materials. Application of this method resulted in discovery of new, formerly unknown



regularities, controlling the substructure nonuniformity in metal materials both after plastic deformation and thermal treatment [2-5].

It was found that, depending on the orientation of reflecting planes, the physical half-width of the registered X-ray line can vary from 10 to 15 angular minutes up to 1.5 to 2 degrees and even higher. The actual upper limit of line broadening is beyond reach for detection, since usually the wider is the X-ray line the lower are both its intensity and the measurement accuracy. Hence, in the same sample the substructure condition of crystallites varies within a very wide range: side by side with large blocks, having the relatively perfect lattice, there is a fraction, characterized by extremely small coherent domains and/or the utmost lattice distortion. When comparing positions of maxima and minima in GPF I_{hkl} and GPF 2_{hkl} , it becomes evident that minima of line broadening coincide with texture maxima, whereas maxima of line broadening are localized within texture minima. In other words, the dispersity of coherent domains and the lattice distortion are minimal in texture maxima and increase up to highest values by passing to texture minima. This is the most general rule, controlling the substructure inhomogeneity of textured materials. Substructure differences between texture maxima and texture minima are explained on the basis of texture formation models by use of the concepts of orientation stability, successive retardation and activation of slip systems, fragmentation of grains due to fluctuations of their orientation about the stable position.

It becomes evident by consideration of GPF 2_{hkl} (or GPF d_{hkl}/d_{av}) for deformed materials, that the interplanar spacing d_{hkl} changes continuously, when passing from one region of GPF to another, differing in the orientation of reflecting planes. Hence, the concept of interplanar spacing as applied to textured samples has a sense only on condition that it is determined as a distribution. Moreover, an

inhomogeneous distribution of d_{hkl} has place not only in deformed polycrystals, but even in rolled single crystals with the sharp one-component texture. As a result of rolling, within the single crystal two subcomponents prove to be formed, close by orientations and differing in types of elastic deformation (extension or compression) along the same cubic axes.

A common feature of GPF 2_{hkl} (or GPF d_{hkl}/d_{av}) is the cross-wise pattern, consisting in alternation of quadrants with opposite predominant signs of elastic deformation. It is seen that zones of extension and compression tend to be aligned parallel with texture maxima at their opposite slopes. When the rolling texture is multi-component and shows significant scattering, the distribution of lattice elastic deformation loses partially its clearness and becomes more complicated. But even in these cases a predominance of extensive or compressive microstrains remains evident within alternating quadrants of GPF. The revealed regularity of inhomogeneous microstrain distribution provides the equilibrium of residual microstresses in rolled textured materials and can not be predicted by mental models.

1. Yu. Perlovich, H.J. Bunge, M. Isaenkova, *Text. & Microstr.*, **29** (1997), 241-266.
2. Yu. Perlovich, H.J. Bunge, M. Isaenkova, V. Fesenko, *Text. & Microstr.*, **33** (1999), 303-319.
3. Yu. Perlovich, H.J. Bunge, M. Isaenkova, *Z. Metallkd.*, **91** (2000), 2, 149-159.
4. Yu. Perlovich, M. Isaenkova, *Met. Mat. Trans. A*, **33A** (2002), 867-874.
5. Yu. Perlovich, M. Isaenkova, *Mat. Sci. Forum*, **443-444** (2004), 255-258.

B1 - O3

NON-DESTRUCTIVE PHASE ANALYSIS AND RESIDUAL STRESSES MEASUREMENT BY GRAZING ANGLE X-RAY DIFFRACTION GEOMETRY

S. J. Skrzypek¹, J. Jeleńkowski², W. Ratuszek¹, T. Wierzchoń²

¹Faculty of Metallurgy and Materials Science, University of Mining and Metallurgy, Al. Mickiewicza 30, 30-059 Kraków, Poland, e-mail:skrzypek@uci.agh.edu.pl, fax: (48) 12 6173190

²Faculty of Materials Science, University of Technology, 02-507 Warszawa, ul. Wołoska 141. Poland

The non destructive structure characterisation of surface layers for various kind of fatigue experiments and machining of heat-treated steels and stainless steels or other materials having metastable phase can be a powerful tool in surface engineering. These kinds of treatments can cause phase transformation and/or non-uniform plastic deformation in surface layer. It is connected with volume change and non-uniform elasto-plastic deformation, which create residual macro and/or micro-stresses. These characteristics are gradient-like in mostly similar cases.

An application of classical X-ray diffraction \sin^2 method and classical Bragg-Brentano diffraction geome-

try in these kinds of examinations make some problems in term of X-ray real depth of penetration. The Bragg-Brentano diffraction geometry is characterised by parallel diffracting crystallographic planes $\{hkl\}$ to the surface and non-linear increase of effective depth of X-ray penetration when Bragg angle (θ) increases, contrary when \sin^2 method is used. An application of $g\text{-}\sin^2$ method which is based on grazing angle X-ray diffraction geometry made possible to get real value of residual macro-stresses and additionally could be suitable in estimation of their gradient-like distribution. An application of this geometry to X-ray diffraction phase analysis enabled

to get phase contents versus thickness under surface in non-destructive way.

Surface preparation is usually demanded treatment like grinding and/or polishing before coating deposition. The grinding and polishing of austenitic steel can cause phase transformation of austenite and non-uniform plastic deformation in surface layer.

The X-ray quantitative phase analysis was used to establish volume fraction of transformed austenite. Theoretic-

cal calculation of residual macro-stresses due to volume fraction of transformed austenite in stainless steel and following measurements of residual stresses were carried out as well.

Grinding and polishing of samples caused big compressive residual stresses and phase transformation of austenite in thin surface layer. These factors can influence on properties of following deposited coatings.

B1 - O4

X-RAY SCATTERING FROM INTERFACE DISLOCATIONS IN HIGHLY MISMATCHED OXIDE EPITAXIAL FILMS

R. Guinebretiere, A. Boulle, O. Masson, A. Dauger

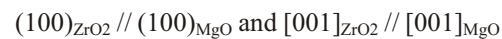
Science des Procédés Céramiques et de Traitements de Surface, UMR 6638. ENSCI, 47 Av. A. Thomas 87065 Limoges, France

It is well known that the real physical properties of thin films are often greatly influenced by the microstructural characteristics of the film. Among microstructural parameters the state of strain of the film is probably one of the most important. During the last decade a large amount of work has been devoted to the determination of strains and strain gradients in epitaxial thin films. Nevertheless, most of the studies are related to semiconductor or metallic thin films. Since several years we are developing specific x-ray diffraction setup and modeling tools dedicated to the study of nanostructured oxide materials [1, 2]. The main specificity of those materials is that they exhibit high defect densities as compared to semiconductor materials.

In epitaxial thin films strains are generally related to the lattice mismatch across the film – substrate interface. The strain distribution is therefore highly anisotropic and moreover non constant along the normal to the interface. Recently, we proposed a new approach of the description of the strain gradient in epitaxial thin films [3]. This approach, based on the use of B-spline functions, allows one to obtain a precise description of the strain evolution along the normal to the interface. Experiments were performed on 60 nm thick epitaxial zirconia thin films deposited on sapphire substrate. As a result, we observed a strongly diverging behavior occurring near the interface in the first 5 nm of the film [3]. In comparison with the work done on semiconductor thin films we could imagine that such behavior is related to the presence of misfit dislocations. In this communication we give further evidence of the presence of such dislocations and discuss the possible effects on the XRD profiles.

The first step in such a study is to choose a convenient sample. Previous TEM studies on ZrO_2 thin films grown on MgO showed that this system exhibits a simple cube on cube epitaxy [4,5]. The samples were elaborated through a specific sol-gel process already described elsewhere [4]. A thermal treatment of the samples at 1500°C during one hour induces the formation of zirconia islands epitaxied onto the magnesia substrate. The epitaxial relationships between zirconia island and magnesia substrate where con-

firmed through x-ray diffraction scans and ω -scan. Those relationships are the followings:



The structure of the interface as been studied by high resolution x-ray diffraction. Reciprocal space maps (RSM) were measured using a specific x-ray diffraction setup already described in details [1,2]. The two dimensional intensity distributions were obtained in a one step measurement procedure. In spite of a large broadening of the reciprocal lattice points (RLP), those measurements were performed in only few hours. For instance, a RSM including the (200) magnesia RLP and the (200) zirconia RLP is given figure 1. According to the well known orientation conventions, Q_z is perpendicular to the interface and Q_x is lying in the interface. We recorded such maps at different values of the θ angle and for two orders of the (h00) zirconia planes.

The mean thickness of the islands was determined by line profile analysis performed on q_z sections of the (200) and (400) zirconia RSM. This mean thickness is close to $t = 100\text{nm}$ and the root mean squared strain is 0.044%.

In the MgO/ZrO₂ system the theoretical lattice mismatch is close to 20% and strain relaxation is therefore highly expected in particular through the generation of misfit dislocations. The presence of dislocations lying at the interface must induce modification of the scattering profile in the Q_x direction. A section along this axis, of the (200) zirconia RLP is given figure 2a. This scan exhibit a peculiar line shape made of two symmetrical shoulders around the main peak. It should be noticed that such line shapes have already been observed by other authors in sample containing misfit dislocations [6, 7].

The understanding of the physical meaning of the presence of those satellites requires the comparison of several scans obtained for several reflection orders. The transverse scan of the (400) zirconia RLP is reported figure 2b. The two satellites are also clearly visible. An interesting feature is that both profiles are perfectly superimposed (after rescaling by a constant factor) on an angular scale. This

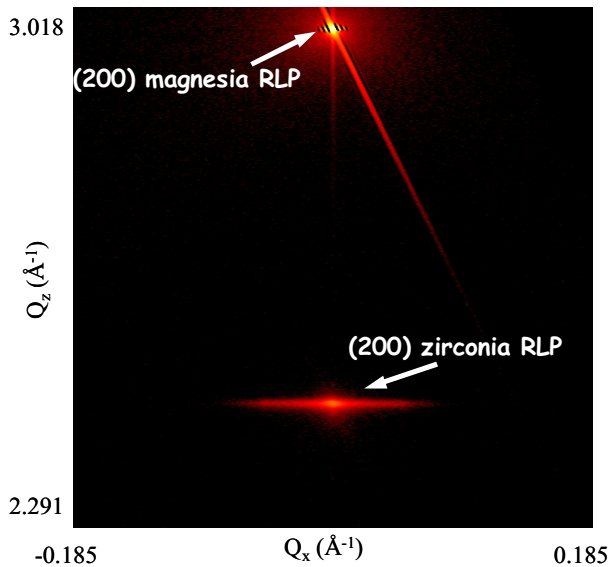


Figure 1: Reciprocal space map including the (200) zirconia RLP and the (200) magnesia RLP.

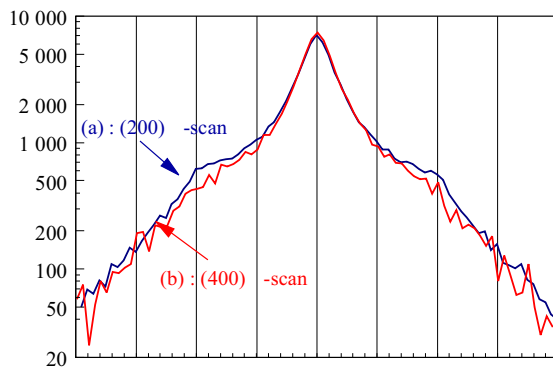


Figure 2: transverse scans of the (h00) reciprocal nodes. (a) q_x scan across the (200); (b) q_x scan across the (400).

B1 - O5

EXPERIMENTAL ANALYSIS OF SHOT PEENING INDUCED RESIDUAL STRESSES IN STEEL SAMPLES

P. Sedlák^{a,1}, N. Ganev^{a,2}, L. Berka^{b,3}

^a Faculty of Nuclear Sciences and Physical Engineering, CTU in Prague, Czech Republic

^b Faculty of Civil Engineering, CTU in Prague, Czech Republic

¹ sedlak@troja.fjfi.cvut.cz, ² ganev@troja.fjfi.cvut.cz, ³ berka@fsv.cvut.cz

The aim of this contribution is to present a comparative analysis of macroscopic residual stress distribution in the surface layers of shot-peened steel samples by means of X-ray diffraction and semi-destructive ring cutting technique.

Shot peening process consists of the controlled bombardment of the metal surface by spherical shot including steel shot, steel and stainless steel pieces of wire, ceramic or glass beads. The shots may be driven by a high velocity stream of air or liquid or by mechanical device in which the

demonstrates that the effects responsible for this peculiar line shape are linearly dependent of the order of reflection and no size effect is observed. Such behavior is characteristic of a disorder that is rotational in nature [8]. In particular, the addition (or subtraction) of half planes not perpendicular to the interface (e.g. with a non zero z-component of the Burgers vector) can explain such a behavior. The presence of the two secondary maxima could be related the existence of two equivalent glide planes for those dislocations.

Further details concerning the XRD analysis as well as the possible slip systems will be given at the conference.

1. A. Boulle, O. Masson, R. Guinebreiere, A. Lecomte and A. Dauger. *J. Appl. Cryst.* 35(2002)606-614.
2. A. Boulle, O. Masson, R. Guinebreiere and A. Dauger. Diffraction analysis of the microstructure of materials. Springer Series in Materials Science, vol. 68, 2004, ISBN 3-540-40519-4 Pages 505-526.
3. A. Boulle, O. Masson, R. Guinebreiere, A. Dauger. *J. Appl. Cryst.* 36(2003)1424-1431.
4. R. Guinebreiere, B. Soulestin and A. Dauger. *Thin Sol. Films.* 319(1998)197-201.
5. R. Guinebreiere, A. Dauger, O. Masson and B. Soulestin. *Phil. Mag. A* 79[7](1999)1517-1531.
6. V. M. Kaganer, R. Köhler, M. Schmidbauer, R. Optiz and B. Jenichen., *Phys. Rev. B* 55[3](1997)1793-1810.
7. A. Yu Babkevich, R. A. Cowley, N. J. Mason, S. Weller and A. Stunault. *J. Phys. Cond. Matter* 14(2002)13505-13528.
8. P. F. Miceli and C. J. Palmstrom. *Phys. Rev. B* 51[8](1995)5506-5509.

shots are fed into a rotating wheel and thrown at the desired velocity. The treatment causes plastic flow of the surface layers, thereby inducing surface compressive stresses, change of microstructure and may cause phase transformation in the surface layers.

However, there is not a simple relationship between the parameters of shot peening and the course of residual stresses induced in the surface layers of treated materials [1,2]. Final results of shot peening depends on its conditions and on properties of treated material including

microstructure and crystallographic structure. Therefore reliable methods of experimental stress analysis have to be applied for control of the resultant state of residual stresses.

X-ray diffraction is the most accurate and best developed method of quantifying the residual stresses produced by surface treatments such as shot peening, and the method is widely used in automotive and aerospace applications. X-ray diffraction is applicable to most polycrystalline materials, metallic or ceramic, and is non-destructive at the sample surface.

Classical X-ray methods are limited to relatively fine-grained materials; the most experimental errors are caused by extreme preferred orientation and near-surface stress gradients.

A common *mechanical methods for stresses measuring* involves the removal of stressed materials and measurement of the strain relaxation in the adjacent material [3]. These methods are widely used in industry for many years, mostly the hole drilling method with electrical resistance strain gages. However, they are not straightforwardly applicable for the residual stress determination of shot peened samples because of the steep near-surface stress gradients. The removal area has form of ring in the *ring cutting technique* and the strain relaxation is measured in the centre of the ring. The use of finite element calculation is always needed for the interpretation of results.

Shot peened plates were prepared from steels Cz grade 12050 (sample A), Cz grade 14220 (sample B), Cz grade 19312 (sample C) and PN 17145 (sample D).

A θ -goniometer was used to measure the diffraction line $-Fe \{211\}$. In order to determine the stress gradient beneath the samples surface, the layers were gradually removed by electrolytic polishing.

Distributions of macroscopic residual stresses obtained are plotted in Fig.1. Surface residual stresses (MPa) obtained in two directions $\alpha = 0^\circ$ and $\alpha = 90^\circ$ perpendicular each to another are summarized in the Tab.1.

Tab.1. Surface residual stresses [MPa] obtained by \sin^2 method

Sample	Orientation $\alpha = 0^\circ$	Orientation $\alpha = 90^\circ$
A	-496 42	-485 33
B	-358 15	-363 9
C	-339 12	-319 18
D	-628 36	-676 \pm 72

The stereo-image technique for strain measurement was used at the ring cutting method. The maps of strains were obtained by the stereo-comparison of the images taken before and after the ring cutting process. Stress relaxation was measured in the inner part of the ring. The ring diameters were: inner radius 1.07 mm; depth 3.50 mm; width 1.70 mm. The ring was removed by electric-corrosive process in petroleum bath. The values of stresses were calculated from the maps of shifts using Hook's law.

The results of both methods were compared using the finite element analysis. Tab. 2 shows the comparison of

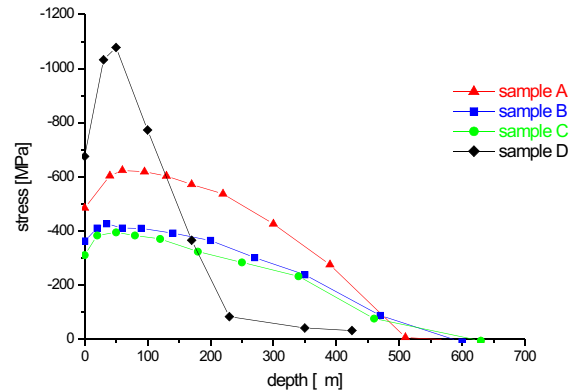


Fig.1. Depth profiles of residual stresses obtained by means of \sin^2 method in the surface layers of shot-peened samples

stresses calculated by finite element model with input from X-ray determined stress profiles with stresses evaluated by the ring cutting method.

X-ray diffraction was found as the most accurate method for quantifying the residual stresses but extremely time-consuming (one depth distribution - about 10 hours) that can be a big disadvantage in the process of quality control testing.

Ring cutting measurement is not so lengthy but, on the other side, does not give any information about depth profile. The values of surface stresses for both methods are in a good agreement despite near-surface stress gradients in samples. Finite element analysis showed us that more detailed analysis of measured shifts in the ring cutting method can give additional information about depth of stressed layer. However, more accurate system for shift measurement is needed.

Tab.2. Comparison of stresses [MPa] evaluated by ring cutting method and calculated by FEM from depth profiles

Sample	Ring cutting method	Calculated by FEM
A	-696 \pm 66	-600
B	-444 \pm 72	-407
C	-241 \pm 54	-381
D	-708 \pm 105	-674

ACKNOWLEDGEMENTS

The research has been supported by the project Grant Agency of the Czech Republic q106/03/1039.

- [1] Kraus, I., Ganev, N.: in *Industrial Application of X-Ray Diffraction*. New York, Marcel Dekker 1999.
- [2] Noyan I. C., Cohen J. B.: *Residual Stresses*, Springer - Verlag, New York 1987.
- [3] Berka, L., Sova, M., Růžek, M., Fischer, G. *Nové možnosti mechanických metod analýzy zbytkových napětí*. Sborník přednášek z 34. konference EAN Plzeň 1996.



B1 - O6

STUDY OF MARTENSITIC TRANSFORMATION IN FATIGUED STAINLESS STEEL BY NEUTRON DIFFRACTION STRESS ANALYSIS

Yu. V. Taran¹, M. R. Daymond², J. Schreiber³

¹FLNP, Joint Institute for Nuclear Research, 141980 Dubna, Moscow region, Russia

²ISIS, Rutherford Appleton Laboratory, Chilton, Oxon OX11 0QX, UK

³EADQ, Fraunhofer Institute for Nondestructive Testing, D-01326 Dresden, Germany

The elastoplastic properties of an austenitic matrix and martensitic inclusions induced during cyclic tensile-compressive loading of low carbon metastable austenitic stainless steel were studied during *in situ* neutron diffraction stress rig experiments on the ENGIN instrument at the ISIS pulsed neutron facility, with the aim of studying the effects of fatigue on the phase elastic stiffness.

Two sets of samples were prepared from the austenitic steel AISI 321. The first set of samples (annealed at 1050 °C and quenched in water) was cycled under strain control with strain amplitude of 1% at a frequency of 0.5 Hz (low-cycled fatigued (LCF) samples). The second set (1070 °C / quenched in air) was cycled under stress control with stress amplitude of 330 MPa at 5 Hz (high-cycled fatigued (HCF) samples).

Subsequent applied stress - elastic strain responses of the austenitic and martensitic phases for both axial and transverse directions relatively the applied load axis were obtained by Rietveld and Le Bail refinements of the neutron diffraction spectra, and were used to determine the elastic constants of the phases as a function of fatigue level.

An unusual phenomenon is observed for both sets of samples, viz. nonlinear behaviour of martensite elastic response in the plastic region, while the austenite elastic response remains linear throughout the measured stress range up to 500 MPa. This effect was interpreted as the additional microstresses induced by the applied load in the martensite phase in the plastic region, providing the most likely mechanism for the unusual strain response of the phase.

Results of LCF-samples study may be summarized in the following way:

- a clear trend of increasing Young's modulus with fatigue level was noted in the austenite matrix;
- the ratios of elastic constants for transverse and axial directions in both austenite and martensite are close to expected based purely on the value of the Poisson's ratio;

- the residual strains in the austenitic matrix were determined as a function of fatigue cycling, using a noncycled sample as a reference sample; a weak tensile strain of the austenite matrix is observed in both directions; such determination for martensite was impossible for lack of a reference sample;

- the residual macrostresses and the deviatoric components of the phase residual microstresses were determined assuming that the elastic properties of both phases are similar; the austenite phase shows a compressive deviatoric stress in the axial direction, while the martensite shows a balancing tensile deviatoric stress in this direction; the magnitude of the austenite deviatoric compressive stress increases with fatigue, however the tensile deviatoric stress in the martensite decreases in magnitude, corresponding to the increasing volume fraction of martensite.

Among results of HCF-samples study note only one more unusual phenomenon in the martensite phase: the axial and transverse elastic constants of austenite and martensite are distinctly different, especially clear in the transverse direction; the ratio of axial and transverse elastic constants for martensite is almost twice that observed (of 0.28) in austenite phase of the HCF-samples and in both phases of the LCF-samples, and that expected based purely on the value of the Poisson's ratio; the mechanism for this unusual behaviour is unclear, but may be linked to the shape of the martensite.

Investigations described in literature have indicated a different morphology of the martensite phase as a function of the cycle frequency; they have also revealed a remarkable difference in the martensite transformation properties between the stress- and strain-controlled tests. We plan to perform series neutron experiments with the aim of clarification of the observed phenomena.